Colloid Polym Sci (2008) 286:917–926
DOI 10.1007/s00396-008-1848-4

ORIGINAL CONTRIBUTION

Growth regimes and spherulites in thin-film poly(ε-caprolactone) with amorphous polymers

Yu-Fan Chen · E. M. Woo

Received: 30 November 2007 / Revised: 29 January 2008 / Accepted: 4 February 2008 / Published online: 21 February 2008

Abstract Spherulite ring-band patterns and growth regimes in neat poly(ε-caprolactone) (PCL) and its miscible blends were analyzed using polarized-light optical microscopy and differential scanning calorimetry (DSC). Spherulite growth in thin-film forms and transformation of spherulite patterns in different regimes were investigated by comparing neat PCL with its miscible blends. Three miscible diluents in PCL were probed: poly(*p*-vinyl phenol) (PVPh), poly (benzyl methacrylate) (PBzMA), and poly(phenyl methacrylate) (PPhMA), which represent strong H-bonding and weak polar interactions, respectively. Blending of PCL with miscible amorphous polymers changes the spherulite patterns significantly. The effect of different diluent polymers varies. Inclusion of different amorphous polymers in PCL leads to different extents of suppression in growth rates and induces different spherulitic patterns. The H-bonding interaction leads to that the PCL/PVPh blend shows dendritic crystals and no ring bands. Although PPhMA differs from PBZMA only by a methylene in the chemical structure of repeat unit, the coil-like textures of ring bands in the PCL/PPhMA blend are widely different from the zig-zag ring bands in the PCL/PBzMA blend. Regime plots show that the growth of neat PCL behaves quite differently from any of its blends with amorphous polymers (PVPh, PPhMA, or PBzMA). Regime plots for PCL/PBzMA blend also differ from those for the PCL/PPhMA blend, which correlates with the crystal patterns seen in these two blend systems.

Y.-F. Chen · E. M. Woo (✉)
Department of Chemical Engineering,
National Cheng Kung University,
Tainan 701, Taiwan
e-mail: emwoo@mail.ncku.edu.tw

Keywords Crystallization regime · PCL · Blends

Introduction

Polymers in thin-film forms can behave differently from bulk forms. Crystalline morphology of polymers in thin films can display unusual patterns such as complex ring bands or dendrites instead of regular Maltese-cross spherulites. The patterns can be further influenced by factors such as film thickness, temperature range, or types of amorphous diluent polymers. Patterns of crystalline spherulites in polymers can depend on the structures, geometry restriction in growth, or temperatures of crystallization, etc. Ring band, Maltese cross, and dendrite are three patterns often seen in various situations. In some vinyl polymers (e.g., polyethylene; or poly(vinylidene fluoride)) [1–4], the Maltese-cross pattern can be seen along with concentric extinction ring bands in spherulites. Extinction ring patterns are also seen in several aryl or aliphatic polyesters [5–8], as well as occasionally in some other polymers [9–12].

Growth and patterns of spherulites in film forms of polymers can be quite different from those found in bulk forms, owing to difference in growth geometry restriction. Peculiar dendritic crystal forms have been reported in various polymers in ultra-thin films (nano-scales), such as iPS, poly(ethylene oxide) (PEO), etc. Kinetic-related diffusion restriction in ultra-thin confinement is usually proposed as a mechanism responsible for the formation of dendritic (rather than round-shaped spherulites) crystals [13]. In addition to dendritic crystals occasionally found in ultra-thin-film forms of polymers, ring-band patterns in spherulites growing on thin-film planes (film thickness in micron scales) have been intriguing. Mechanisms of edge-on vs. flat-on lamella [14] or spiraling lamella [15] owing

to internal stresses, etc., have been proposed. Hong et al. [16], in investigating crystal growth in PTT, observed that spherulite patterns were different from one regime to other, in which they have claimed that ring-banded spherulites are observed in regime II, while ring-less Maltese-cross spherulites are in regime III. More recently, however, a concurrent work on acryl polyesters has led to a new frontier that kinetic regime transitions can signal several complex pattern transformations in spherulites, not simply just transition from ring-less to ring-banded spherulites, or vice versa [17]. Crystallization kinetics and spherulite growth mechanism have been extensively studied on semicrystalline polymers, such as poly(ε-caprolactone) (PCL) [18, 19], PVF_2 [20], and PEO [21–24], etc., or their blends with amorphous polymers. Influencing factors may include molecular weight (MW), MW fractions, miscibility, and copolymer or blend composition, etc, which are the focal points of many studies [1–7]. These factors happen to also influence the patterns of spherulites, such as ring bands, regularity of rings, patterns of ring order, etc. Thus, regime kinetics may be in correlation with transformation of spherulite patterns.

The spherulites in PCL are normally ring-less when crystallized at most T_c. Ring-banded spherulites in PCL are seen only when crystallized at high T_c (closer to T_m) and the ring bands are usually of low regularity with highly zig-zag patterns; however, blending of miscible diluents with PCL tends to change the patterns of spherulites. PCL spherulites in neat PCL have been reported to be distinctly different from those in miscible PCL/poly(benzyl methacrylate) (PBzMA) and PCL/poly(phenyl methacrylate) (PPhMA) blends [25, 26]. Ring bands become more distinct and orderly in miscible PCL blends with amorphous polymers, and ring bands can usually form at lower T_c's in blends than neat PCL, owing to either depressed T_m or elevated T_g in blends by presence of the amorphous polymer. In this study, PCL and its blends composed of different amorphous polymers were chosen as models for comparative studies on relationships between kinetic regimes and spherulite patterns. They were targeted for such study objectives for comparative reasons probing effects of types of miscible diluents on growth rates and patterns of crystals developed.

Experimental

Materials and procedures

PCL was purchased from Aldrich Chem. Co., with weight-average molecular weights (M_w) of 20,000 g/mol. The glass transition temperature and melt point for PCL are −70 and 60 °C. Three different amorphous polymers used to blend with PCL are as following. PBzMA and PPhMA were obtained from Scientific Polymer Products, Inc. PBzMA was purchased from Scientific Polymers Product, Inc. (USA), with manufacturer data of M_w=51,000 g/mol with polydispersity index (PI)=2.67 (GPC), and a T_g of 54~60 °C. Our laboratory characterization showed a more exact M_w=54,000 g/mol (GPC) and PI=2.27, and T_g (onset) of 57.2 °C for the PBzMA. PPhMA, supplied from Scientific Polymer Products, Inc. (USA), has an approximate MW=100,000 g/mol (GPC), and a T_g of 105~110 °C. Poly(*p*-vinyl phenol) (PVPh) was obtained from Polysciences, Inc. (USA) with T_g=148 °C. These three amorphous polymers were chosen because they can all form miscible blends with PCL [25–28], but with different interaction strengths. PVPh interacts with PCL in blends via H-bonding [28] but the polymethacrylates (PBzMA and PPhMA) do not. The different interaction modes in blends make ideal models for comparison in evaluating effects of interaction strength on growth kinetics and spherulite patterns.

Blends of two polymers, one being polyester PCL and another being an amorphous polymer (PVPh, PBZMA, or PPhMA) of intended compositions, were prepared via solvent-blending using proper solvents. Blending using several different solvents was attempted. It was finally determined that tetrahydrofuran (THF) yielded the best result and was used for preparing samples of both blend systems investigated in this study. The polymers were first weighed respectively and dissolved into the solvent with continuous stirring with a stirrer or magnet. Subsequently, the resulting polymer solution was poured into a flat mold kept at 45 °C. The solvent in the cast film samples was first vaporized under a hood at a controlled temperature, followed by de-gassing in a vacuum oven for 48 h at 50~60 °C. Polymer solutions were then cast on glass substrates forming a film of samples with controlled thickness. Average thickness of the cast films (for neat polymers or blends) was estimated to be 5 μm or less, but no thinner than 2 μm.

Apparatus and procedures

T_g transitions of the blend samples were measured with a differential scanning calorimeter (DSC-7, Perkin-Elmer) equipped with an intracooler (to −60 °C) and data acquisition/analysis. Additional sub-ambient DSC runs (as low as −100 °C) were cooled with a liquid nitrogen tank and helium gas purge. Prior to DSC runs, the temperature and heat of transition of the instrument were calibrated with indium and zinc standards. During thermal annealing or scanning, a continuous nitrogen flow in the DSC sample cell was maintained to ensure minimal sample degradation.

Radial growth of spherulites was recorded and rates measured using a polarized optical microscopy (POM, Nikon Optiphot-2) equipped with a temperature-controlled

hot stage and a Nikon charge-coupled device (CCD) digital camera and automatic image-processing software. In preparing OM samples, neat PCL or its blend in solvent (THF) was cast onto glass slides as thin films (3~5 μm) for OM characterization and measurement of growth rates. A drop of 4% solution of the polymer (or blends) was deposited and uniformly spread on a glass slide and the solvent was allowed to fully evaporate in an atmosphere. The films with a free surface upward were first melted on one hot stage at 90 °C for 5 min and then were rapidly transported to another hot stage controlled at T_c. Spherulite patterns were taken and recorded at selected temperatures as functions of time. The size and growing rate of the growing spherulites were measured via image-processing software for automatic interval recording of morphology, which provided automatic calibration of the magnification to actual dimensions.

Results and discussion

Growth regimes of neat PCL in comparison with blends

Figure 1 shows spherulite growth rates (G in μm/min measured along radial direction) as functions of T_c for thin films of PCL and blends with various amorphous polymers at different crystallization temperatures. The growth rates differ for neat PCL and its blends with various amorphous polymers, PVPh, PPhMA, or PBzMA, of three compositions. Neat PCL has the greatest growth rate than all blends at a fixed T_c, indicating reduction of growth rates by any of the diluent polymers. PPhMA tends to have higher tendency for reducing the growth rates of PCL in blends when compared to PBzMA at the same T_c and composition. One then wonders if the difference in reduction on growth rate has any effect on the spherulite patterns. This will be analyzed in following sections.

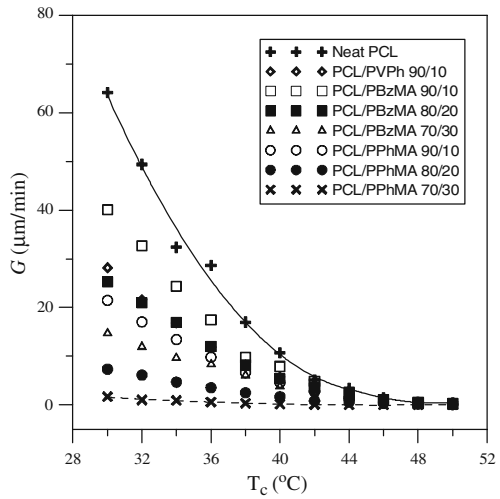

Fig. 1 Crystal growth rates for PCL and blends with various amorphous polymers at different crystallization temperatures

By following the regime analysis of the Lauritzen–Hoffman (L–H) model, the growth rate of a crystallizing polymer during crystallization is described as [29, 30]:

$$G = G_o \exp\left[\frac{-U^*}{R(T_c - T_\infty)}\right] \exp\left[\frac{-K_g}{T_c(\Delta T) f}\right] \quad (1)$$

where U^* is the activation energy of the molecular transferring through the melt–crystal surface, T_∞ is the temperature at which the transport of segments across the liquid–solid interface becomes infinitely slow, and K_g is the activation energy of nucleation for a crystal. The f factor is a correction coefficient for the temperature dependence of enthalpy of fusion, ΔH_f^o.

$$f = 2T_c/\left(T_m^o + T_c\right)$$

The nucleation constant K_g can be expressed as:

$$K_g = \frac{n_e b_o \sigma \sigma_e T_m^o}{\Delta H_f^o \kappa} \quad (2)$$

where n_e is a constant equal to 4 for regime I and III, and 2 for regime II; b_o is the thickness of monolayer (film) in the direction normal to the growth plane; σ is the lateral-surface free energy; and κ is the Boltzmann constant. It is usually more convenient to re-write Eq. (1) to a logarithmic form for plotting:

$$\ln G + \frac{U^*}{R(T_c - T_\infty)} = \ln G_o - \frac{K_g}{T_c \Delta T f} \quad (3)$$

Where K_g can be obtained by plotting the left-hand side of Eq. 3 versus $1/(T_c\,\Delta T\,f)$. Table 1 lists the DSC-determined values of T_g and equilibrium melting temperatures of neat PCL and PCL blends with amorphous polymers of various compositions to be used in regime calculations. Standard procedures for determination of equilibrium melting temperatures were used; for brevity, the detailed DSC traces and procedures for extrapolating to T_m^o are not shown here.

Neat PCL was first investigated as a base for comparison with its miscible blends. Figure 2 shows Lauritzen–Hoffman plots and morphology for neat PCL in regimes II and III, respectively. Inset graphs show that the Maltese-cross spherulite is featured in regime III, where the spherulites (T_c=30~45 °C) are mostly Maltese-cross with no ring bands. Slope change signals a transition in growth. At the temperature of transition (46 °C), where two straight lines intersect, the spherulite is still Maltese-cross but starts to display coarsened lamella at slightly higher T_c. Then, in regime II (T_c>46 °C), dendrites with highly irregular ring-band patterns are seen, where ring-bands patterns superimposed on dendritic spherulites are seen only at high T_c of 52~54 °C. Dendritic characteristic with ring-band steadily

Table 1 T_g and equilibrium melting temperatures of neat PCL and blends of various compositions to be used in regime calculations

	wt./wt.	T_g (°C)	T_m^o (°C)
Neat PCL		−70	64
PCL/PVPh	90/10	−60	61.76
PCL/PBzMA	90/10	−67.4	63.36
	80/20	−64.11	62.9
	70/30	−58.91	61
PCL/PPhMA	90/10	−65.4	62.5
	80/20	−62.5	61
	70/30	−54.5	60.5

increases with T_c within regime II. For neat PCL, rough and barely identifiable ring bands are seen at high T_c; by contrast, when crystallized at lower T_c's, the spherulites in PCL are mostly ring-less. A transition temperature is seen to locate at about 46 °C (marking a division between regime II and III), where the spherulite pattern transforms from Maltese-cross (for T_c lower than 47 °C) to dendrite (feather-like) types with irregular zig-zag rings (for T_c higher than 47 °C).

PCL/PVPh blend

Blending of PCL with miscible amorphous polymers resulted in significant changes in the spherulite patterns. PCL/PVPh blend is known to be miscible with a strong H-bonding specific interaction [28], and the interaction parameter for the PCL/PVPh blend measured by the melting point depression method is $\chi_{PCL-PVPh}=-1.508$ [27]. Spherulitic morphology and kinetic regime behavior for neat PCL was compared to those in the PCL/PVPh blends of a representative composition (w/w=90/10). Figure 3 shows the Lauritzen–Hoffman plot covering regime II and III for the PCL/PVPh (90/10) blend. Inset graphs show different patterns in spherulites melt-crystallized at temperatures of regimes. Striking differences in the spherulite patterns are seen between the neat PCL and PCL/PVPh blend. For the PCL/PVPh (90/10) blend, spherulites are seen to become dendritic in crystallization from T_c=35~45 °C (regime III); whereas for neat PCL, a very high T_c>55 °C is needed to develop dendrites. The strong interaction between PCL and PVPh likely counts for the change. Regime kinetics transition is quite obvious as the slope change is distinct between two regimes, and an intersecting point is located at T=46 °C, which is nearly the same as that for neat PCL. Slope change signals a transition in growth, as well as crystal pattern. At T_c above the transition point, dendrites become more apparent and increase in the leaf size for blends crystallized at increasingly higher temperatures, from T_c= 46~55 °C (regime II). Higher crystallization T_c greater than 55 °C led to too slow growth kinetics for the blend morphology to be conveniently monitored. At higher loadings of PVPh (>10 wt.%) in PCL blends, dendrites become increasingly larger and more apparent. For brevity, morphology for PCL/PVPh blends of higher PVPh loadings is not shown. Physical changes induced by PVPh in PCL are mostly: (1) elevation of T_g, and (2) depression of T_m of PCL, and (3) interactions between crystallizing species and diluent, which all may contribute to the observed changes in the regime growth and spherulite patterns. Strong H-bonding between PCL and PVPh favors slow growth of dendritic crystals and likely leads to cancel the formation of ring bands in PCL. In an earlier study [31], blends of PCL with tannic acid (TA), a tri-phenol bio-resourceful species, also results in dendrites and similar disruption of ring-band patterns as that observed for the PCL/PVPh blend.

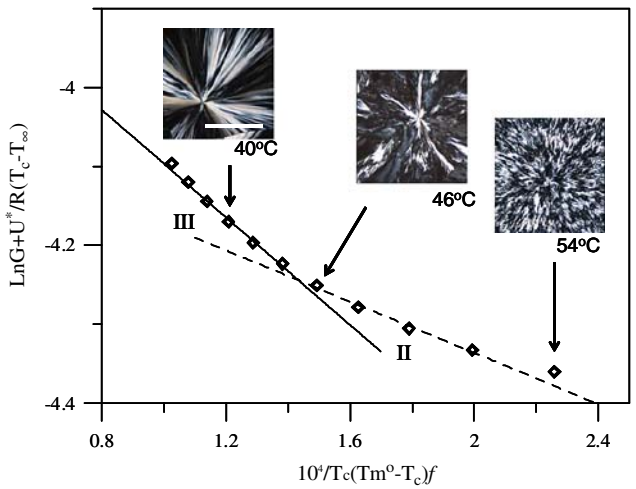

Fig. 2 Regime III and II crystallization plots of PCL by employing U^*=1,500 cal/mol. *Inset*: representative spherulite patterns illustrated at different regimes

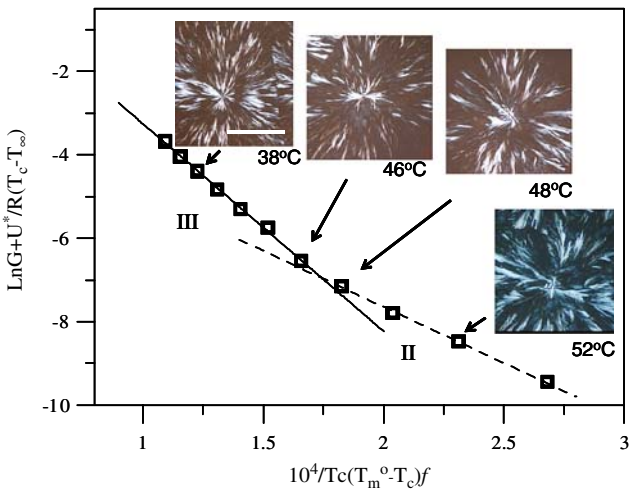

Fig. 3 Regime II and III crystallization of PCL/PVPh=90/10. Representative spherulite patterns illustrated at two different regimes

PCL/PBzMA blend

Blend of PCL/PBzMA is known to be miscible via weak-to-moderate polar–polar interactions between the backbone ester group of PCL and the pendant acrylate ester group of PBzMA [25, 26]. From a previous study [26], the interaction parameters have been determined to be $\chi_{PCL-PPhMA}=-0.40$ (or $B_{PCL-PPhMA}=-1.997$ cal cm^{-3}) at 60 °C for PCL/PPhMA. For PCL/PBzMA, the parameter has a lower value of $\chi_{PCL-PBzMA}=-0.22$ (or $B_{PCL-PBzMA}=-0.96$ cal cm^{-3}) at 60 °C. Both values are a lot smaller than that for the PCL/PVPh blend. Spherulitic morphology and kinetic regime behavior were investigated for PCL/PBzMA blends of several representative compositions. Ring bands in spherulites of PCL/PBzMA blends of three compositions (*w*/*w*=90/10, 80/20, and 70/30) were apparent at all isothermal temperatures of crystallization in the range 30–55 °C. Major features of ring bands in the PCL/PBzMA blend appeared to be significantly different from those in neat PCL or the PCL/PVPh blend discussed in previous figures. This fact indicates that patterns of ring bands may be influenced by the nature of the amorphous polymers blended with PCL, where interaction strength may vary with respect to types of diluents in PCL. Figure 4 shows Lauritzen–Hoffman plot covering regime II and III growth for the PCL/PBzMA (90/10) blend. Inset graphs show corresponding patterns of spherulites melt-crystallized at temperatures of different regimes. Ring bands in spherulites of the PCL/PBzMA (90/10) blend are seen in regime III of all T_c (30~55 °C). Regime transition is present but less obvious as the slope change is minor between two regimes; nevertheless, an intersecting point is located at T=44 °C. Below T_c=44 °C, regime III is characterized with ring-band spherulites, while regime II above 44 °C is featured with ring-less spherulites and become increasingly dendritic with

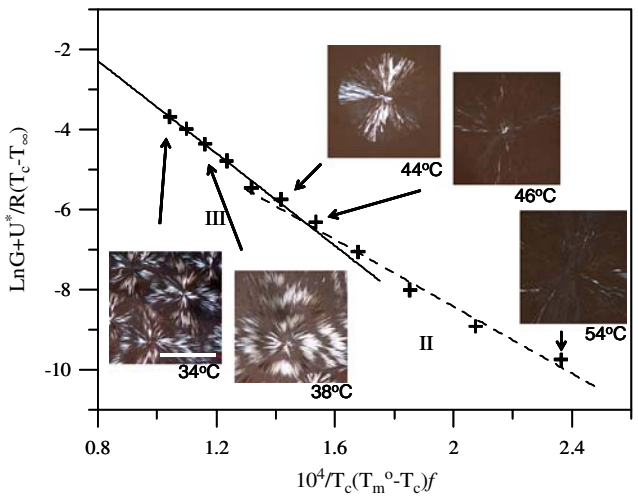

Fig. 4 Regime III and II growth for the PCL/PBzMA (90/10) blend. Representative spherulite patterns illustrated at two regimes

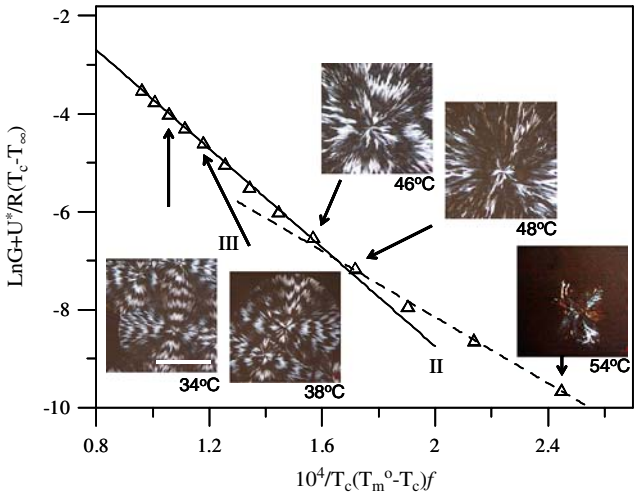

Fig. 5 Regime III and II growth of PCL/PBzMA (80/20) blend. Representative spherulite patterns illustrated at two different regimes

higher T_c. Note that this pattern in the PCL/PBzMA blend is opposite to the trend in neat PCL, where regime III is featured with ring-less Maltese-cross spherulites and regime II dendritic/ring-banded spherulites, as discussed in the previous figure.

It was of interest to examine the effect of higher loadings of PBzMA in the blends. PCL/PBzMA blends of two other compositions with higher amorphous PBzMA contents were also examined (80/20 and 70/30). Figure 5 shows regime II and regime III plot of PCL/PBzMA (80/20) blend. Inset graphs show patterns of spherulites melt-crystallized at different regimes. Distinct ring-band spherulites are seen at all T_c (30~45 °C) in regime III for the PCL/PBzMA (80/20) blend. The spherulites in the blends are ring-banded for all T_c's in regime III; in contrast, neat PCL displays no ring bands in regime III. Ring bands are apparent and orderly concentric in the blend, especially when crystallized at increasingly higher T_c up to 45 °C. For the PCL/PBzMA (80/20 wt. ratio), regularity of the ring bands is generally higher than that seen in the PCL/PBzMA (90/10) blend. Regime kinetics transition is apparent that signals a slope change between two regimes, with an intersecting point at T=~46 °C.

PCL blend with PBzMA at 30 wt.% loading was further examined for comparison. Figure 6 shows regime II and III plot of PCL/PBzMA (70/30) blend. Inset graphs show different patterns in spherulites melt-crystallized at corresponding temperatures of regime. For this blend, regime kinetics transition is seen with an intersecting point located at T=46 °C. Below T_c=46 °C, regime III is characterized with ring-band spherulites, while regime II above 46 °C is featured with ring-less spherulites. With further increase in T_c, the ring-less spherulites become increasingly dendritic. Again, ring bands in spherulites of PCL/PBzMA (70/30) blend are still apparent and easily recognizable when

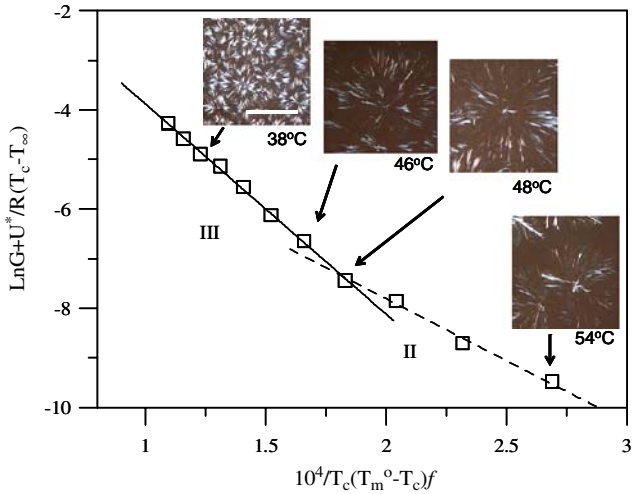

Fig. 6 Regime III and II growth of PCL/PBzMA (70/30) blend. Representative spherulite patterns illustrated for two regimes

crystallized at all T_c (30~55 °C). However, the spherulites of the PCL/PBzMA (70/30) blend in general become smaller than those seen in the PCL/PBzMA (80/20) blend, and rings in this blend are less ordered too. In general, ring patterns are the most clearly visible and ordered in the PCL/PBzMA blend of *w*/*w*=80/20 composition, and regularity in ring bands decreases with either increase or decrease from 80/20 composition in the diluent contents in blends. Inclusion of 20 wt.% amorphous PBzMA in the PCL blends leads to most distinct or regular ring bands in spherulites; incorporation of greater fractions of amorphous polymer (30 wt.% or higher) in the PCL blends leads to increasing disruption or eventual disappearance of ring bands in spherulites.

PCL/PPhMA blend

PPhMA differs from PBzMA only by a methylene in the chemical structure of repeat unit; however, interaction type between PCL and PPhMA is similar to that between PCL and PBzMA via weak C=O polarity. Three compositions of PCL/PPhMA blend (90/10, 80/20, 70/30) were examined and are discussed separately. Figure 7 shows Lauritzen–Hoffman plot and spherulite patterns of PCL/PPhMA (90/10) blend. Inset graphs show patterns in spherulites melt-crystallized at temperatures of regime III (lower T_c= 35~45 °C) and regime II (higher T_c>45 °C). Ring bands, in general, are more orderly spaced in the spherulites of the PCL/PPhMA blend than those found in the PCL/PBzMA blend of same compositions. By referring to the counterpart plots for the PCL/PBzMA (90/10) blend discussed earlier in previous figure, the PCL/PPhMA (90/10) blend exhibits more orderly ring bands in the spherulites at the same T_c than does the PCL/PBzMA (90/10) blend. For this blend, regime kinetics transition is seen with an intersecting point located at T=~46 °C. Below T_c=46 °C, regime III is characterized with ring-band spherulites, with ring regularity decreasing with increasing T_c. A slope change is seen at T_c=46 °C, where regime II above T_c=46 °C is featured with dendritic but ring-less spherulites.

Figure 8 shows a Lauritzen–Hoffman plot of PCL/PPhMA (80/20) blend. Inset graphs show changing patterns of spherulites in the blend melt-crystallized at specific temperatures of regimes. Again, ring bands are seen in the spherulites of the PCL/PPhMA (80/20) blend when crystallized in regime III (lower-T regime). For this blend composition (80/20), ring bands are all highly irregular and of a zig-zag pattern, with irregularity increasing with T_c in this temperature range (regime III: 30~45 °C). Note that at T_c=45 °C, the PCL/PPhMA (80/20) blend exhibits highly thickened and zig-zag ring bands and that the Maltese-cross pattern either disappears or is masked by the highly thickened/rough bands. The plot shows that at higher temperatures, a slope change signals a transition to regime

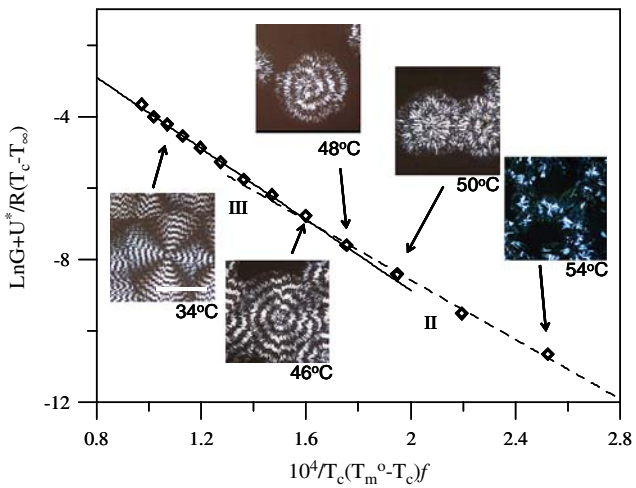

Fig. 7 Regime III and II growth of PCL/PPhMA (90/10) blend. Representative spherulite patterns illustrated at two different regimes

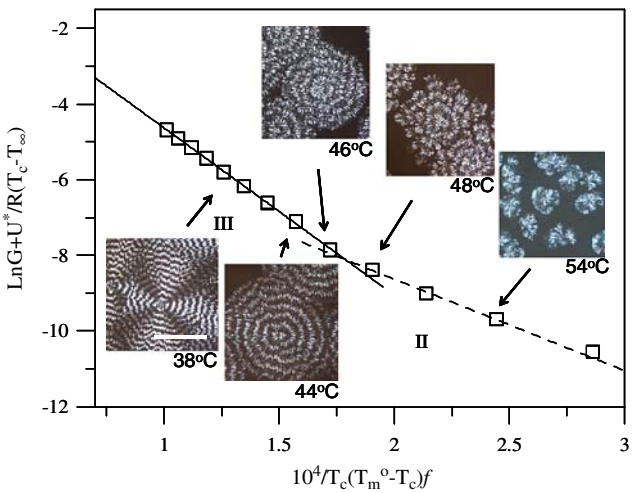

Fig. 8 Regime III and II crystallization of PCL/PPhMA (80/20) blend. Representative spherulite patterns illustrated at different regimes

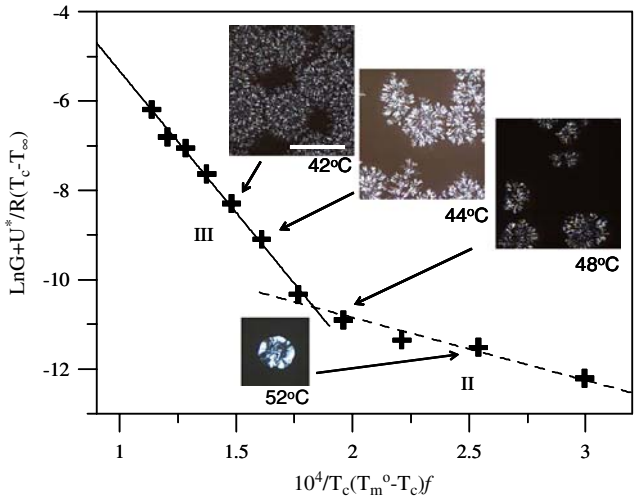

Fig. 9 Regime III and II crystallization of PCL/PPhMA (70/30) blend. Representative spherulite patterns illustrated at different regimes

II, where spherulite growth is slow and no ring bands are present in the spherulites.

Figure 9 shows Lauritzen–Hoffman plot and spherulite patterns of PCL/PPhMA (70/30) blend, which also displayed regime II and III. Inset graphs show corresponding pattern in spherulites melt-crystallized at temperatures of regime (30~48 °C). For this composition (70/30) crystallized at T_c of regime III (30~48 °C), ring bands are all of a peculiar coil-like pattern with irregularity increasing with T_c in the temperature range. The coil-like ring bands appear to be an overlap of both coils and short dendrites fanning out along the rims of concentric rings. Note that the ring-band pattern in the PCL/PPhMA blends is unique and dramatically different from those seen in either neat PCL, PCL/PVPh, or PCL/PBzMA blend. In most T_c range of regime III (33~48 °C), the spherulites of the PCL/PPhMA (70/30) blend exhibits highly thickened coil-like ring bands with no Maltese cross bisecting the spherulites, except for the blend sample crystallized at the lowest T_c of 30 °C (whose spherulites shown as inset graph at far-left of the figure). At higher T_c within regime II (T_c>48 °C), growth became very slow, and only small Maltese-cross spherulites were seen after long time.

Effects of different diluents on growth and spherulites

As shown earlier in Fig. 1, all PCL blends exhibit suppressed growth rates in comparison to the neat PCL, with the suppression extent increasing with contents of the amorphous polymer in the blends. PPhMA, among the three diluents investigated, tends to exert the most depression effect on the growth rates of PCL in blends when compared at same T_c and same diluent loadings. Inclusion of different amorphous polymer in PCL tends to lead to different ring patterns, as it is clear that the ring bands in the PCL/PPhMA (90/10, 80/20, 70/30) blend differ from those in the PCL/PBzMA blend (90/10, 80/20, 70/30) in regularity, band width, and inter-ring spacing, as well as general patterns of spherulites, etc. The growth data in the figure show that at 10 wt.% amorphous diluent loading in blends do not differ much from diluent to diluent. Inclusion of moderate 10~15 wt.% amorphous polymer (PPhMA or PBzMA) in the PCL blends may be inductive for forming most distinct, regular or compact ring bands in spherulites. PPhMA contents of 20 or 30 wt.% in the PCL/PPhMA blend are noted to cause more extreme suppression of growth rates in comparison to the PCL/PBzMA blend of the same diluent loadings. Especially, the inclusion of PPhMA greater than 20 wt.% in the PCL blends leads to dramatically different ring bands in regime III, and different dendritic spherulites in regime II from those seen in the PCL/PBzMA blends.

The effect of PPhMA is similar to PBzMA on the PCL spherulites in blends in that ring patterns are similarly induced in regime III; however, there are significant differences in the spherulite patterns. Patterns of ring bands in spherulites of PCL/PPhMA blend are distinctly different from those seen in two other blend systems (PCL/PVPh or PCL/PBzMA). When crystallized at low T_c in regime III, the ring bands in PCL/PPhMA blend are more distinct and more orderly arranged as concentric rings than those seen in the PCL/PVPh or PCL/PBzMA blends, where ring bands are either ill-defined, hard to recognized, or highly zig-zag. Again, major features of ring bands in the PCL/PPhMA blend appeared to be significantly different from those in the PCL/PBzMA blend, which, in turn, differed significantly from those in the PCL/PVPh blend. Ring bands in the PCL/PPhMA blend are mostly not zig-zag but quite orderly spaced, unlike those highly distorted zig-zag ring patterns in the PCL/PBzMA or PCL/PVPh blend. When compared at the same T_c (in regime III) and same amorphous polymer loading of 10 wt.%, the inter-ring spacing and band width are narrower and smaller in the PCL/PPhMA blend than those in the PCL/PBzMA, which, in turn, exhibit much thinner bands and smaller inter-ring spacing than the PCL/PVPh blend. These differences provided positive evidence that the patterns of ring bands are influenced by nature of the amorphous polymers blended in PCL.

Figures 10 (a and b) shows summary plots of ln $G+U^*/R(T_c-T_\infty)$ vs. $1/T_c(\Delta T)f$ for neat PCL in comparison with (a) PCL/PBzMA and (b) PCL/PPhMA blends of three compositions. Regime plots have been separately shown in previous figures. This figure simply summarizes all systems on the same coordinates for comparison. The regime plots show that the growth of neat PCL behaves quite differently from any of its blends with amorphous polymers (PVPh,

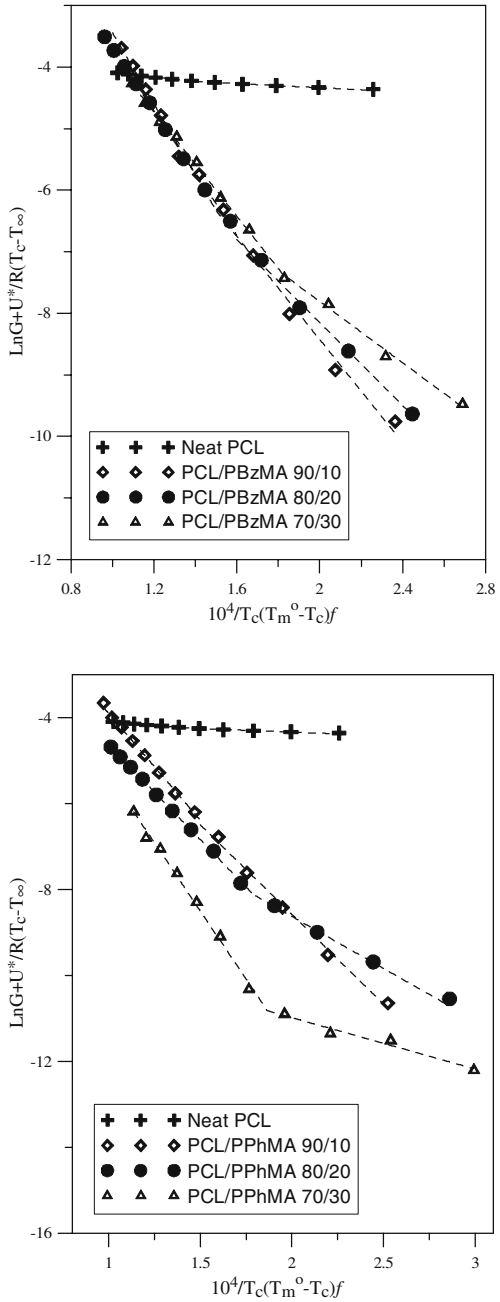

Fig. 10 Summary plots of ln $G+U^*/R(T_c-T_\infty)$ vs. $1/T_c(\Delta T)f$ for neat PCL in comparison with blends of **a** PCL/PBzMA and **b** PCL/PPhMA (three compositions)

PPhMA, or PBzMA). Furthermore, the regime plots for PCL/PBzMA blend also differ from those for the PCL/PPhMA blend, and this fact correlates with the significantly different crystal patterns seen in these two blend systems. Table 2 shows the kinetic values obtained from the regime calculations. For comparison, T_g of neat PCL and calculated T_g of its blends with three diluent polymers of various compositions (by using the Fox equation: $1/T_g=w_1/T_{g1}+w_2/T_{g2}$) are also listed. T_g variation among the various systems is within 15 °C, and T_m^o variation is no more than 3 °C. In fitting the growth data, a value of $U^*=1{,}500$ cal/mol was used for neat PCL and its blends. The slopes of regime plots yield values of K_g. Ratio of K_{gIII}/K_{gII} reflects slope change from regime II to III, which is nearly 2 for neat PCL but varies from 1.2 to 1.85 for most blends except for the PCL/PPhMA (70/30) blend.

Discussion

Regime transitions are commonly observed for many polymer systems; however, pattern changes of the spherulite/lamellae in different regimes are not always similar. A few examples are cited here for comparisons. Roitman et al. have reported the regime transition crystallization and morphology of poly (pivalolactone) [32]. They observed that spherulites formed at higher temperatures of regime II and quenched to room temperature exhibit concentric-ring "cracks", whereas the spherulites formed at lower temperatures of regime III and quenched to room temperature do not exhibit such concentric cracks. They claim that this fact indicates that the chain folding is more regular in regime II than in regime III in accordance with the nucleation theory, but the authors did not discuss any correlation of crystal morphology with respect to regime behavior. Similar discussions about isotactic polypropylene were made by Cheng et al. [33], who observed gradual morphological changes not in correlation with regime transitions; instead, the birefringence gradually diminishes from wholly positive to slightly positive in regime III but, by contrast, it changes to a slightly negative birefringence with transition from regime III to II. A kinetic analysis by Doi et al. on the crystal growth in poly(L-lactic acid) (PLA) in thin-film forms demonstrated regime transitions from regime III to regime II and from regime II to regime I [34]. According to their study, a transition from regime II to I induces a morphological change in the crystallized aggregates, whereby initially spherulitic aggregates can be transformed into hexagonal lamellae stacks. They claim that, for transition between regimes II and III, no obvious morphological change in the

Table 2 Kinetic values obtained from regime calculations

System	wt./wt.	K_{gIII}	K_{gII}	K_{gIII}/K_{gII}	$T_{III\rightarrow II}$ (°C)
Neat PCL		3,405	1,622	2.10	45
PCL/PVPh	90/10	49,716	26,893	1.85	47.2
PCL/PBzMA	90/10	57,754	41,860	1.38	45.5
	80/20	50,403	33,689	1.50	47.1
	70/30	42,395	24,883	1.70	47.9
PCL/PPhMA	90/10	49,705	41,697	1.19	46.5
	80/20	44,193	24,194	1.83	46.8
	70/30	63,420	14,060	4.51	46.75

spherulitic/crystal aggregates is present. For linear polyethylene, Hoffman et al. [35] reported that transition from regime I to regime II is quite sharp (in slope change) and is accompanied by a change in structures from axilites to spherulites. Hoffman and Miller in 1989 have summarized in a communication a list of references on regime kinetic transitions for various polymers into two main types: (1) regime I to II, and (2) regime II to III; but no structural changes in the polymers are discussed [36]. The results of these above classical studies have shown that variety of patterns of crystal spherulites/aggregates in semicrystalline polymers may be present in different regimes of growth; however, no rules seem to be applicable for predicting specific patterns in going through regimes of kinetic growth. Transitions and accompanying changes in crystal structures from spherulites to different shapes of crystal aggregates are widely reported in classical literature; however, few address changes in ring bands structures in corresponding transition of kinetic regimes. This study provides timely probes to fill up the inquiry gap.

Conclusions

Spherulite growth in thin-film forms and transformation of spherulite patterns in different regimes were investigated by comparing neat PCL with its miscible blends. Effect of different diluent polymers varies. Blending of PCL with miscible amorphous polymers changes the spherulite patterns significantly. For neat PCL, in transition from regime III to regime II, the spherulites are patterned in ring-less to ring-banded types, respectively, in different regimes. Maltese-cross spherulites and dendritic crystals (with highly irregular ring bands and no Maltese cross) are featured in different growth regimes (low- and high-temperature regimes, respectively) in neat PCL. Regime growth transition signals a corresponding transition in spherulite patterns (from Maltese-cross to dendritic). All Maltese-cross spherulites and most dendrites are not ring-banded. Only the dendrite spherulites in PCL grown at extremely high temperatures are ring-banded (those formed at T_c of 52~54 °C or higher), in which the dendritic spherulites are featured with rough and irregular ring bands. Two regimes (III and II) are generally observed in neat PCL or its miscible blends. For neat PCL, the spherulites transform from ring-less Maltese-cross pattern (in regime III) to ring-banded (with rough dendrites) at higher temperatures of regime II.

Inclusion of different amorphous polymers in PCL leads to different extents of suppression in growth rates and induces different spherulitic patterns. Mechanisms of such changes involve several factors such as nature of the polymers in blends exhibit difference in the interaction strength, which influence the growth kinetics, leading to difference in the spherulite patterns. Transition of regimes does not necessarily signal a change from ring-less to ring-band, or vice versa, but it does correlate with a change in the spherulite patterns. Slope change reflects different growth kinetics (nucleation control or molecular diffusion control, etc.), where difference in spherulite morphology resulted from a difference in growth kinetics. The PCL/PBzMA and PCL/PPhMA blends exhibit a similar regime transition, but completely different spherulite patterns from those in neat PCL. The PCL/PBzMA blend shows spherulites in orderly ring bands at lower T_c (regime III), and become ring-less at higher T_c (regime II) and eventually dendritic at even higher T_c. By comparison, the PCL/PPhMA blend exhibits similar transition of spherulite patterns from regime III to II. However, the textures of ring bands in the PCL/PPhMA blend are different from those in the PCL/PBzMA blend. PBzMA and PPhMA are similar amorphous polymer species with the same carbonyl ester group. The difference in ring-band textures may result from difference in interactions between PCL and PBzMA or PPhMA. On the other hand, blending with miscible amorphous polymers with strong interactions significantly tends to prohibit formation of ring bands, but favors formation of dendritic crystals.

Acknowledgment This work was financially supported by a basic research grant (NSC-94 2216 E006 003) in three consecutive years from the *National Science Council* (NSC) of Taiwan.

References

1. Keith HD, Padden FJ (1984) J Polymer 25:28–42
2. Lovinger AJ, Keith HD (1996) Macromolecules 29:8541–8542
3. Keith HD, Padden FJ (1996) J Macromolecules 29:7776–7786
4. Keller A (1955) J Polym Sci 17:291–308
5. Wang J, Lin CY, Hanzlicek J, Cheng SZD, Geil PH, Grebowicz J, Ho RM (2001) Polymer 42:7171–7180
6. Hu YS, Liu RYF, Zhang LQ, Rogunova M, Schiraldi DA, Nazarenko S, Hiltner A, Baer E (2002) Macromolecules 35:7326–7337
7. Ho RM, Ke KZ, Chen M (2000) Macromolecules 33:7529–7537
8. Wu PL, Woo EM (2003) J Polym Sci Part B: Polym Phys 41: 80–93
9. Wang Z, An L, Jiang W, Jiang B, Wang X (1999) J Polym Sci Part B: Polym Phys 37:2682–2691
10. Keith HD (1982) Macromolecules 15:122–126
11. Keith HD, Padden FJ Jr, Russell TP (1989) Macromolecules 22:666–675
12. Lotz B, Thierry A (2003) Macromolecules 36:286–290
13. Zhai X, Wang W, Zhang GL, He BL (2006) Macromolecular 39:324–329
14. Lovinger AJ (1980) J. Polym Sci Polym Phys Ed 18:793
15. Lotz B, Cheng SZD (2005) Polymer 46:577–610
16. Hong PD, Chung WT, Hsu CF (2002) Polymer 43:335–3343
17. Chen YF MS thesis, Dept Chem Engn, National Cheng Kung University, Tainan, Taiwan (2007)

18. Kressler J, Svoboda P, Inoue T (1993) Polymer 24:3225–3233
19. Chen HL, Li LJ, Ou-Yang WC, Hwang JC, Wong WY (1997) Macromolecules 30:1718–1722
20. Wang TT, Nishi T (1977) Macromolecules 10:421–425
21. Maclaine JQ, Booth C (1975) Polymer 16:191
22. Keith HD, Padden FJ Jr (1986) Polymer 27:1463–1471
23. Alfonso GC, Russell TP (1986) Macromolecules 19:1143–1152
24. Beech DR, Booth C, Hillier IH, Pickles CJ (1972) Euro Polym J 8:799
25. Woo EM, Mandal TK (1999) Macromol Rapid Commun 20:46–49
26. Woo EM, Mandal TK, Lee SC (2000) Colloid Polym Sci 278:1032–1042
27. Kuo SW, Huang CF, Chang FC (1998) J Polym Sci Polym Phys 39:1348–1359
28. Coleman MM, Moskala EJ (1983) Polymer 24:251–257
29. Hoffman JD, Weeks JJ (1962) J Res Natl Bur Stand, Sect A 66:113
30. Hoffman JD, Davis GT, Lauritzen JI (1976) In: Hannay NB (ed) Treatise on solid state chemistry. Plenum, New York Vol 3, Chap 7
31. Yen KC, Mandal TK, Woo EM (2007) J Biomed Mater Res, accepted
32. Roitman DB, Marand H, Millar RL, Hoffman JD (1989) J Phys Chem 93:6919–6926
33. Cheng SZD, Janimak JJ, Zhang A, Cheng HN (1990) Macromolecules 23:298–303
34. Abe H, Kikkawa Y, Inoue Y, Doi Y (2001) Biomacromolecules 2:1007–1014
35. Gedde UW (1995) Polymer physics. Chapman Hall, London, p 184 Chap 8
36. Hoffman JD, Miller RL (1989) Macromolecules 22:3502